JOURNAL OF MOLECULAR RECOGNITION
J. Mol. Recognit. 2004; **17**: 397–407
DOI:10.1002/jmr.694

Macromolecular crowding in biological systems: hydrodynamics and NMR methods‡

Pau Bernadó[1]†, José García de la Torre[2] and Miquel Pons[1]*

[1]Departament de Química Orgànica, Universitat de Barcelona, Martí i Franquès 1-11 and Laboratory of Biomolecular NMR, Parc Científic de Barcelona, Josep Samitier 1-5, 08028 Barcelona, Spain
[2]Departamento de Química Física, Facultad de Química, Universidad de Murcia, 30071 Múrcia, Spain

Most biologically relevant environments involve highly concentrated macromolecular solutions and most biological processes involve macromolecules that diffuse and interact with other macromolecules. Macromolecular crowding is a general phenomenon that strongly affects the transport properties of macromolecules (rotational and translational diffusion) as well as the position of their equilibria. NMR methods can provide information on molecular interactions, as well as on translational and rotational diffusion. In fact, rotational diffusion, through its determinant role in NMR relaxation, places a practical limit on the systems that can be studied by NMR. While in dilute solutions of non-aggregating macromolecules this limit is set by macromolecular size, in crowded solutions excluded volume effects can have a strong effect on the observed diffusion rates. Hydrodynamic theory offers some insight into the magnitude of crowding effects on NMR observable parameters. Copyright © 2004 John Wiley & Sons, Ltd.

Keywords: **NMR; rotational diffusion; translational diffusion; NMR relaxation; protein–protein interactions; macromolecular crowding**

Received 25 November 2003; revised 16 February 2004; accepted 18 February 2004

INTRODUCTION

Macromolecular crowding effects change the solution properties of a molecule by virtue of the volume excluded by high concentrations of macromolecular co-solutes. High concentrations of macromolecules are found in the cell cytoplasm, extracellular matrix and even in some physiological fluids. For example, the concentration of protein and RNA molecules in the cytoplasm of *Escherichia coli* is 300–400 g l^{-1} (Zimmerman and Minton, 1991) and they occupy 20–30% of the total cellular volume; blood plasma contains 80 g l^{-1} of protein. Crowding effects have been known for a long time but their relevance to biological systems is often overlooked. General reviews include those by Zimmerman and Minton (1993) and Ellis (2001a,b).

The fraction of volume available to macromolecular solutes, as defined by the possible locations of its centre of mass that are not forbidden by steric overlap with co-solutes, decreases with increasing molecular size. Excluded volume effects depend on the size, shape and concentration of co-solutes and on the size and shape of the molecule of interest.

Excluded volume effects are, by definition, universal and non-specific and will be present in addition to specific interactions, attractive or repulsive, between particular sets of molecules in solution. In the 'moderately crowded region', where collisions between macromolecules are not very frequent, the predominant effect should be solvent-mediated interaction between particles, rather than direct particle-particle or excluded volume interaction. The usual approach to represent the former interaction is by means of the hydrodynamic theory of particles immersed in a continuous solvent, in which motion of particles is coupled by hydrodynamic interactions.

When the molecular weight of the macromolecular co-solutes increases to the point that they can be considered effective immobile obstacles forming a lattice with pores that can be occupied by the molecular species of interest, molecular crowding is referred to as molecular confinement. The background lattice may or may have not some long-range order. In an ordered lattice, excluded volume effects may result in partial orientation of the solute molecules.

Major qualitative effects of macromolecular crowding include:

(1) Shifts in the position of equilibrium processes that lead to more compact species. This includes macromolecular association (e.g. oligomerization, protein–protein or protein–DNA interactions) and conformational changes (e.g. protein folding or DNA compaction).

*Correspondence to: M. Pons, Departament de Química Orgànica, Universitat de Barcelona, Martí i Franquès 1–11, 08028 Barcelona, Spain.
E-mail: mpons@ub.edu
†Present address: Institut de Biologie Structurale Jean-Pierre Ebel, 41 Rue Jules Horowitz, Grenoble 38027, France.

‡This paper is published as part of a special issue entitled 'EMBO Workshop on Biological Implications of Macromolecular Crowding held on 14–18 June 2003, Las Navas del Marqués, Avila, Spain'.

Contract/grant sponsor: Spanish Ministerio de Ciencia y Tecnología; *contract/grant numbers:* BIO2001-3115; BQU2003-04517.
Contract/grant sponsor: Generalitat de Catalunya.

Abbreviations used: BPTP, bovine protein tyrosin phosphatase; HI, hydrodynamic interaction; HMQC; heteronuclear multiple quantum coherences; SE, stimulated echo; TROSY, transverse relaxation optimized.

(2) Decreases in molecular diffusion (rotational and, most specially, translational diffusion), transport properties and diffusion limited reaction rates.
(3) Compartmentalization and supramolecular organization derived from confinement by cellular structures. The resulting spatial organization may have a strong influence on the establishment of intermolecular order and in the efficiency and regulation of metabolic processes.

NMR spectroscopy has repeatedly demonstrated its power to study structure and dynamics of macromolecules in solution. The non-invasive character of NMR and the transparency of biological materials to the radio frequency fields used have led to a spectacular development of NMR methods for the spectroscopic study of living organisms, in addition to its well-known capabilities as an imaging method.

In this article we shall discuss some general principles relevant to the use of NMR to study crowding effects in the three major areas mentioned above.

IN CELL NMR

Macromolecular structure determination by NMR has made isotopic labelling widely available. In the context of macromolecular crowding, isotopic labelling allows the observation of a particular species in the presence of an arbitrary number of other, unlabelled, species without the need of chemical labelling, e.g. by fluorescent tags. In combination with protein overexpression, ^{15}N labelling has allowed the observation of ^{1}H-^{1}N HSQC spectra of several proteins in living *E. coli* cells (Serber and Dötsch, 2001). The quality of the spectra obtained bear witness to the relatively high mobility of these proteins in the *E. coli* cytoplasm.

Specific effects related to macromolecular crowding have been detected by comparing spectra of the protein FlgM, an 'intrinsically disordered' protein in *E. coli* cytoplasm, diluted solutions and artificially crowded samples in which the protein was studied in the presence of high concentrations ($400\,g\,l^{-1}$) of glucose, ovoalbumin or bovine seroalbumin (BSA). HSQC spectra indicative of a folded form were obtained in the artificially crowded systems and in *E. coli* cells, while the spectra obtained in diluted solution corresponded to a disordered protein (Dedmon *et al.*, 2002).

Not all overexpressed proteins of comparable size give good quality in cell NMR spectra. Interaction with cell structures or with high molecular weight components, such as chaperones or DNA can increase the effective correlation time for rotational diffusion and the transverse relaxation rate, leading to broadening of the NMR signals beyond detection.

Additional factors potentially leading to broad NMR lines include local field inhomogeneities and chemical exchange processes. Local field inhomogeneities arise from magnetic susceptibility gradients within the sample affecting specially compartment boundaries. These effects can be reduced by spinning the sample at the magic angle even at relatively low speed. This approach has been applied in the *in vivo* observation of ^{13}C labelled periplasmic glucan of *Ralstonia solanacearum* (Wieruszeski *et al.*, 2001).

HYDRODYNAMIC MOTION OF PARTICLES UNDER CROWDED CONDITIONS

Hydrodynamic theory has been successfully used to model numerically the rigid body motion of macromolecules of arbitrary shape (García de la Torre *et al.*, 2000; Bernadó *et al.*, 2002b) and to derive the expected heteronuclear NMR relaxation rates. In addition to Brownian interactions with the solvent particles, at high concentrations, the motion of a particle can include interactions with neighbouring macromolecules, via solvent-mediated interactions (hydrodynamic interactions, HI) or by direct interactions. The relative motion of the particles in the system defines a time scale separating the two regimes

(1) At short times, much smaller than the typical time between collisions (See the Appendix), the particle moves in a typical Brownian fashion, with a diffusivity that differs from the free (infinite dilution) Brownian motion due to the HI effect: the particle feels the presence of other nearby particles even if they are at some distance, but does not collide with them in this time scale. Quantitatively, this effect may be important, but does not introduce qualitative differences from the free-particle diffusion. The relative configuration of neighbouring particles defines the instantaneous environment that determines the motion of a particle. At times shorter than the time needed for a molecule to diffuse a distance comparable to the square of its radius, this configuration can be considered static.
(2) In a longer time scale, the distribution of neighbouring particles is not constant and the trajectory of the particle will be determined by collision with other particles, or caging effects. The classical microscopic description of Brownian motion is not valid. The diffusion still can be macroscopically Fickian, but the validity of microscopic laws is suspect. The diffusion coefficients will be mainly determined by non-hydrodynamic effects.

The characteristic times that separate the two regimes depend on the size of the particle under study, other co-solutes and the occupied volume.

The shortest time is given by the characteristic times of (free) translational and rotational Brownian motion of the test particles. For translation, the characteristic time can be defined as the time for which the root-mean-square displacement is the same as the particle size, represented by the spherical radius r_p. The relationship is $r_P^2 = 6(k_B T/6\pi\eta r_P)\tau_{trans}$ so that $\tau_{trans} = \pi\eta r_P^3/k_B T$, where k_B is the Boltzmann constant, T is the temperature and η is the solvent viscosity. For rotation, the characteristic time is the Debye rotational (correlation) time of the spherical particle, $\tau_{rot} = 4\pi\eta r_P^3/3k_B T$. It is evident that these two times are quite similar. However, for a system formed by particles of different sizes, rotational diffusion of a small particle in the presence of much larger co-solutes may take place under conditions in which the larger molecules may be effectively considered static. This situation is likely to be applicable to the rotational reorientation of molecules

that can be studied by NMR in natural crowded systems, like the cytoplasm of the cell.

The kinetics of encounters can be described in terms of the Smoluchowski theory of diffusion controlled reactions (see the Appendix). The collision time is given by:

$$\tau_{col} = [3(k_B T/6\pi\eta)(r_P + r_C)(1/r_P + 1/r_C)\phi]^{-1} r_C^3 \quad (1)$$

where r_p and r_c are the radii of the protein of interest and the cosolute, respectively, ϕ is the fraction of occupied volume, η is the solvent viscosity, k_B is the Boltzmann constant and T is the temperature.

The time scale at which the effects of collision between macromolecules become important can be estimated by comparing the interval between collisions with the characteristic time of translational free Brownian motion ($\tau_{part} = \tau_{trans}$). In a monodisperse solution, τ_{trans} is also the characteristic time for changes in particle distribution.

The short time regime occurs when the collision time is much longer than the particle's characteristic time, $\tau_{col} \gg \tau_{part}$, or when $\tau_{part}/\tau_{col} \ll 1$. Interestingly, the ratio is proportional to the occupied volume fraction, and the proportionality constant is a simple function of the ratio of radii, $\lambda = r_P/r_C$:

$$\tau_{part}/\tau_{col} \approx \phi F(\lambda) \quad (2)$$

where

$$F(\lambda) = (1/2)(1 + \lambda)(1 + \lambda^{-1})\lambda^3 \quad (3)$$

This result can be used for an elementary discussion of the effect of the size ratio on the crowding effect, and employed to determine the limit between the two regimes. For an spherical particle with a radius of 2 nm in a background BSA (MW 66 000; $r_C = 2.75$ nm) particles occupying 30% of the solution volume, the ratio τ_{part}/τ_{col} takes a value of 0.23, probably in the frontier between the two regimes. For a particle of 1 nm of radius, τ_{part}/τ_{col} is 0.036, indicating that rotational diffusion is governed by hydrodynamic parameters. For a particle of $r = 4$ nm, $\tau_{part}/\tau_{col} = 1.9$, indicating that its dynamics would be dictated by collisions with background molecules.

TRANSLATIONAL DIFFUSION AND CROWDING

Translational self-diffusion, or tracer diffusion, is related to the mean square displacement of a single particle per unit time. This is the quantity that is measured by pulse field gradient NMR techniques, as well as with optical techniques such as fluorescence recovery after photobleaching or fluorescence correlation spectroscopy. In a uniform medium the translational self-diffusion coefficient is inversely proportional to the medium viscosity and, for a spherical particle, to the particle radius. The presence of co-solutes occupying a non-negligible amount of the solution volume results in a decrease in the observed diffusion.

For small molecules diffusing in a crowded medium formed by uniform, inert, hard spheres, the observed diffusion coefficient is reduced because of the obstruction effect of the spherical obstacles that force the molecule to diffuse along complicated trajectories. The observed diffusion coefficient, D^t, is related to the one observed in pure solvent, D^t_o, by:

$$D^t = D^t_o(1/1 + 0.5\phi) \quad (4)$$

where ϕ is the fraction of excluded volume. The limiting value for spherical particles is 0.667 D_o. For elongated crowding particles, obstruction effects are more pronounced. Additional reduction in the observed translational diffusion coefficients can be related to binding effects between the diffusing molecule and its co-solutes.

Diffusion of macromolecules is further hindered because of the volume excluded by the diffusing species, by direct interaction between this species and the crowder, and by hydrodynamic interactions. One particular simple case is when the diffusing species and the crowder are the same species and can be considered as hard, inert, spheres.

Translational diffusion coefficients both in the short and the long time regimes have been calculated theoretically and, truncated to the first order in ϕ, follow eqs (5) and (6) (Dhont, 1996).

$$D^t_{short} = D^t_o(1 - q_{short}\phi) \quad q_{short} = 1.83 \quad (5)$$

$$D^t_{long} = D^t_o(1 - q_{long}\phi) \quad q_{long} = 2.11 \quad (6)$$

Experimental evidence provides a value of $q_{long} \approx 2.3$ in good agreement with the theoretical results (Imhof and Dhont, 1995; van Blaaderen *et al.*, 1992; van Megen and Underwood, 1989). The validity of equations (5) and (6) extends up to values of ϕ close to 0.5. For random packed identical spheres ϕ is 0.64.

From a practical point of view it is interesting that the coefficients of ϕ in the two equations are not very different and close to the value expected for diffusion in the long time regime in the absence of hydrodynamic interaction (Hanna *et al.*, 1982):

$$D^t_{long} = D^t_o(1 - q_{NH}\phi) \quad q_{NH} = 2.0 \quad (7)$$

The similarity of the coefficients confirms that, in the long time regime, translational diffusion is dominated by direct particle interactions. On the other hand, in the short time regime, hydrodynamic interactions are totally responsible for the observed dependency of the diffusion coefficient on the fraction of excluded volume.

Alternative expressions for the calculation of translational diffusion both in the short and long time regimes are given by Tokuyama and Oppenheimer (1994) and Han and Herfeld (1993). Figure 2 compares the predicted dependency of D^t/D^t_o with the fraction of occupied volume according to different models. While different models for short time diffusion give comparable results the agreement between the different models for long time diffusion is lower.

PULSE FIELD GRADIENTS TO MEASURE TRANSLATIONAL DIFFUSION BY NMR

Pulsed field gradient NMR techniques are used extensively to measure translational diffusion. In the presence of a

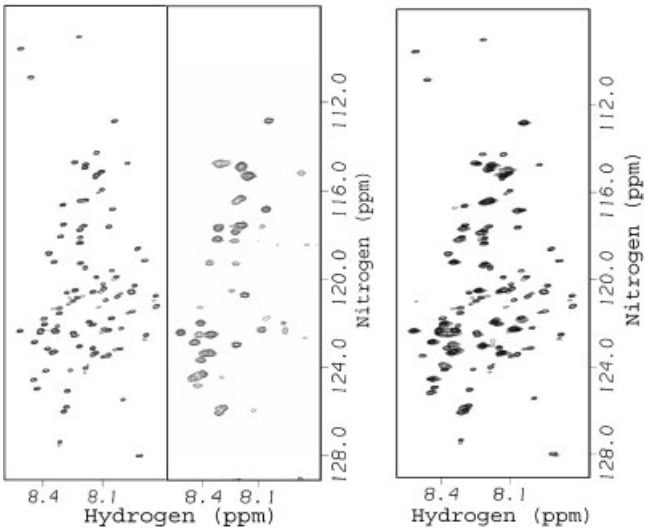

Figure 1. The C-terminal domain of FlgM gains structure in crowded media. In (A) the HN-HSQC spectra of FlgM in diluted solution (left) and in living *E. coli* (right) are compared. A number of signals from the C-terminal part of the protein disappear under crowding conditions. A similar effect is observed when spectra are measured at high concentrations of glucose. In (**B**) spectra recorded at the same concentration of protein in the presence or absence of 450 g L^{-1} glucose are superimposed. The N-terminal domain is mostly unchanged and serves as an internal control. Selective broadening of the C-terminal domain has been interpreted as the result of chemical exchange associated with a folded form that is formed only under crowding conditions. Reproduced with permission from Dedmon *et al.* 2002. Copyright 2002 National Academy of Sciences USA.

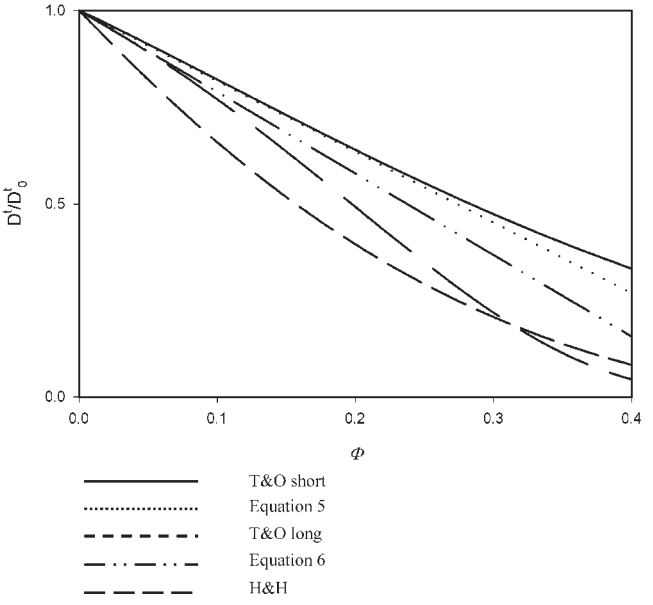

Figure 2. Dependency of reduced translational diffusion coefficients with the fraction of occupied volume according to different models. T&O refers to the model of Tokuyama and Oppenheimer and H&H to the Han and Herzfeld models. T&O short and eq. (5) refer to short time diffusion. T&O long, eq. (6), and H&H are for long time diffusion.

spatially inhomogeneous field (a field gradient), transverse magnetization from nuclei located in different points of the sample acquire different phases. As a result, the signal from the complete sample is effectively averaged to zero. However, the spatial phase encoding induced by a field gradient can be reversed by the application of a second field gradient with exactly the same spatial distribution and intensity but opposite sign. (An equivalent experiment involves the application of identical gradients before and after a 180° pulse that causes the appearance of an echo). The full signal is recovered, except for relaxation effects, provided that the spatial localization of each nucleus does not change between the two gradients. The general experiment is referred to as a pulsed gradient spin echo (PGSE). A number of variations incorporating improvements for known technical problems in the practical implementation of the experiment have been described. For comprehensive reviews see, for example, Johnson (1999) and Price (2000). Diffusion causes an attenuation of the signal that can be described, assuming linear gradients and rectangular gradient pulses, by the Stejskal–Tanner (1965) equation:

$$I(g,\Delta) = Io\ \exp[-\gamma^2\ g^2 D_{\text{trans}}\delta^2(\Delta - \delta/3)] \qquad (8)$$

where γ is the magnetogyric ratio of the nucleus considered, g and δ are the gradient intensity and duration, respectively, Δ is the time delay between the beginning of the two gradients and D_{trans} is the translational diffusion coefficient.

Limitations on the use of PGSE techniques to measure diffusion coefficients in crowded systems are related to the lower limit for the diffusion coefficients that can be measured that depend on the maximum gradient strength and the maximum delay between gradients. Maximum gradient strengths in commercial dedicated instruments are of the order of 20 T m^{-1}. However, typical gradient strengths available in conventional spectrometers are much weaker, less than 0.2 T m^{-1}. Heteronuclear multiple quantum coherences (HMQC) that can be generated easily in isotopically labelled molecules are more sensitive to field gradients, and provide an alternative for the measurement of slow diffusion typical of large molecules or crowded systems (Tillett *et al.* 1999; Kuchel and Chapman, 1993).

The longest value of Δ is determined by attenuation of the signal due to relaxation during the echo time. For molecules with long correlation times, spin-spin relaxations is very effective, thus Δ must be kept as short as possible. Strategies to measure slow diffusion involve the 'storage' of magnetization as long-lived coherences. The most widely used sequences contain variations of the stimulated echo (SE) experiment (Tanner, 1970) in which proton magnetization is stored along the direction of the external field so that the usually slower spin–lattice relaxation is operative for most of the delay. Recently, the X-SE experiment, in which the magnetization is stored as heteronuclear longitudinal magnetization, has been suggested (Ferrage *et al.*, 2003). Spin lattice relaxation of ^{15}N is much longer than for protons allowing an increase in the effective delay between gradients by as much as an order of magnitude. A diffusion coefficient of $(4.99 \pm 0.07)\ 10^{-11}\ m^2\ s^{-1}$ has been measured for the complex tOmpA/C8E4 with a molecular mass of 45 kDa and a rotational correlation time of 20 ns. Spin–spin relaxation during the periods in which gradients are applied

or coherence is transferred will eventually set an upper limit to the measurement of diffusion coefficients of large molecules, although the use of extensive deuteration and transverse relaxation optimized (TROSY) approaches can extend the limit considerably (Pervushin *et al.*, 1997; Pervushin, 2000; Tugarinov *et al.*, 2003).

The presence of intrinsic field gradients in the sample complicates the measurement of diffusion coefficients by NMR (von Meerwall and Kamat, 1989). Nonlinearity in the applied gradients can also give rise to systematic deviations from the Stejskal–Tanner equation similar to those arising from the coexistence of two components with different diffusion coefficients (Håkansson *et al.*, 1977). Intrinsic field gradients, in addition to poor homogeneity of the external field, arise from local differences in magnetic susceptibility in inhomogeneous samples, as for example living cells or other biological samples.

Diffusion in static field gradients can be used as an alternative to the PGSE methods. The main advantage is that static field gradients can be much larger than the pulsed ones. Diffusion in the fringe field of a superconducting magnet allows measurements of diffusion coefficients as small as $10^{-16}\,m^2\,s^{-1}$. The use of very strong gradients also reduces the relative contribution of local gradients (Demco *et al.*, 1994).

ROTATIONAL DIFFUSION

Rotational diffusion can be described by the decay of the autocorrelation function $C(t)$ that relates the orientation of a molecule-fixed vector after a certain time delay. For a spherical molecule in a continuous medium or for diffusion in the short time regime, the decay follows a single exponential that defines the rotational diffusion coefficient. In the long time regime the decay has been shown theoretically (Jones, 1989) to be non-exponential and this has been confirmed experimentally in some cases (Degiorgio and Piazza, 1995) but not in others (Koenderink *et al.*, 2003).

Short time rotational diffusion in concentrated suspensions of uncharged identical hard spherical particles is related to free rotational diffusion in solution by (Cichocki *et al.*, 1999)

$$D^{r}_{short} = D^{r}_{o}(1 - 0.6310\phi - 0.726\phi^2) \quad (9)$$

Compared with the effect of crowding on translational diffusion, rotational diffusion is slowed by a factor around three times smaller.

Average long time rotational diffusion seems to be only slightly slower than D^{r}_{short} to first order in ϕ (Koenderink *et al.*, 2003)

$$D^{r}_{long} \approx D^{r}_{o}(1 - 0.67\phi) \quad (10)$$

As previously observed for translational diffusion, in spite of the fundamental differences between the two time regimes, the relevant diffusion coefficients are similar in both cases.

When spheres of different sizes are considered the theoretical predictions are much less accurate. In binary systems rotational diffusion depends on ϕ and on the ratio λ between the radii of the particle consired r_p and the host crowder spheres r_c (Koenderink *et al.*, 2003):

$$\lambda = r_p/r_c \quad (11)$$

$$D^{r}_{short} = D^{r}_{o}[1 + h(\lambda)\phi] \quad (12)$$

With the theoretical values of $h(\lambda)$ described parametrically by Zhang and Nägele (2002)

$$h(\lambda) = -2.5/(1 + 3.0\lambda^{-1}) \quad (13)$$

Rotational diffusion is strongly slowed with increasing tracer/crowder size ratio λ. In the limit of very large rotating particles it approaches diffusion in a continuous medium with an effective viscosity described by eq. (14):

$$\eta = \eta_o(1 + 2.5\phi) \quad (14)$$

Identically charged spheres are less affected by crowding in the short time regime. Electrostatic repulsion increases the distance between the nearest neighbour particles that are responsible for most of the hydrodynamic interaction effects. The effective size of the rotating particle is larger than the hydrodynamic radius and is concentration dependent. As a consequence, rotational diffusion of charged spheres show a non linear dependency on ϕ (Watzlawek and Nägele, 1997). For monodisperse suspensions

$$D^{r}_{short} = D^{r}_{o}(1 - 1.3\phi^2) \quad (15)$$

This equation is only valid for relatively dilute solutions as long range electrostatic interactions cause a strong correlation between particles. As expected, increasing the ionic strength of the solution shields the electrostatic interaction and causes slower rotational diffusion.

Non-spherical crowders cause, at the same fraction of occupied volume, a larger decrease in rotational diffusion (Koenderink *et al.*, 2003). Hydrodynamic interaction introduces correlation in the orientation of anisotropic particles and favours mutually perpendicular orientations of neighbour elongated particles (Antosiewicz and McCammon, 1995). Hydrodynamic interaction is relatively long range and is comparable to electrostatic interaction (Brune and Kim, 1994). In general, crowding effects are expected to result in higher apparent anisotropy of the diffusing particle as compared with a continuous medium.

ROTATIONAL DIFFUSION AND NMR RELAXATION

Heteronuclear NMR relaxation depends on the modulation of interactions by molecular motion. Excellent reviews provide the reader with the necessary background (Dayie *et al.*, 1996; Korzhnev *et al.*, 2001; Palmer, 2001). For protonated carbon-13 and nitrogen-15 nuclei, the dominant term is usually dipole–dipole interaction with directly bound protons. Modulation of chemical shift anisotropy is also an important relaxation mechanism. Relaxation is effective when modulation takes place at frequencies corresponding to the possible transitions between energy levels in the spin system. These include the resonant frequencies of the nuclei involved and their sum and difference, as well as

the contribution to zero frequency. NMR relaxation measurements are sensitive to reorientation processes taking place in the nanosecond time scale, i.e. in the short time scale for rotational diffusion.

Modulation of molecular motion is a random process with contributions at different frequencies described by the spectral density function $J(\omega)$. The spectral density function is the Fourier transform of the autocorrelation function $C(t)$ that describes the persistence of the orientation of a relevant interaction vector. The orientation of the interaction vector for each resolved spin pair, e.g. the N–H bond vector in a peptide bond in a protein, can often be considered fixed in the molecular frame and the ensemble of N–H bonds senses the motion of the complete molecule in different orientations. For isotropic motion all N–H bonds will sense identical $J(\omega)$. Anisotropic motion can be characterized if the structure of the protein is known. Local motion of the N–H bond introduce an additional modulation which, in general is faster that global reorientation. Fast local motions are often introduced in the form of an order parameter that describes the amplitude of the motion (Lipari and Szabo, 1982a,b). Additional modulation in a slower time scale can take place due to chemical exchange processes (Palmer *et al.*, 2001).

For relatively rigid molecules of known structures the global contribution to relaxation of individual nuclei can be derived from hydrodynamic calculations (García de la Torre *et al.*, 2000). This provides a simple way of detecting fast local motions or exchange processes (Bernadó *et al.*, 2002b).

Slowly reorienting molecules show fast transverse relaxation that results in broad lines and reduced sensitivity. Slow rotational diffusion sets a limit to the systems that can be studied by NMR solution techniques. This limit has been extended recently by the use of extensive deuteration, which decreases dipolar interactions because deuterium has a lower magnetogyric ratio than protons, and by the use of transverse relaxation optimized techniques that make use of destructive interference between different relaxation processes and reduce the transverse relaxation rate, and the linewidths, for certain transitions (Pervushin *et al.*, 1997; Pervushin, 2000; Tugarinov *et al.*, 2003).

Ultraslow rotational diffusion, as occurs in very large colloidal suspensions, can be measured using deuterium NMR. The magnitude of quadrupolar splitting of spin 1 deuterium depends on the orientation of the X–D bond with respect to the magnetic field. Reorientation of the molecule can be measured in an echo experiment in a way formally similar to the measurement of slow chemical exchange. Basically, one measures the probability that an X–D bond changes its orientation by a certain angle during the time between two radiofrequency pulses (Spiess, 1991). The time scale for these experiments exceeds milliseconds and is applicable, for example, to the reorientation of large colloidal particles ($r_t > 100$ nm) in low viscosity solvents.

Rotational diffusion of proteins in the cytoplasm is an important parameter, e.g. for the direct in-cell NMR observation of proteins. Experimental data characterizing rotational diffusion of proteins in the cytoplasm by NMR (Williams *et al.*, 1997; Endre *et al.*, 1983; Livingston *et al.*, 1983) are in agreement with those obtained by other techniques such as electron paramagnetic resonance (Mastro *et al.*, 1984) or fluorescence depolarization (Fushimi and Verkman, 1991; Bicknese *et al.*, 1993; Dayel *et al.*, 1999; Luby-Phelbs *et al.*, 1993; Luby-Phelbs, 1994) These data indicate that the apparent viscosity of the cytoplasm, as measured through rotational correlation times, is increased by a factor of at most 2 with respect to the value obtained in dilute solutions. This fact allows the direct NMR observation of proteins in the cytoplasm (Serber and Dötsch, 2001).

Taking the fraction of occupied volume in the cytoplasm as $\phi = 0.3$, the decrease in rotational diffusion for identical spherical hard particles would be around 25%. The experimentally accessible proteins tend to be smaller than the average macromolecular size in the cell. According to the behaviour in binary systems with $\lambda < 1$, rotational diffusion of spheres smaller than the (average) crowder should be faster. The observed decrease in rotational diffusion for a number of systems suggests that anisotropy of both the diffusing particles and the crowders probably plays an important role. This anisotropy could involve, in addition to shape anisotropy, anisotropic charge distributions and correlated motions of anisotropic particles coupled through long-range hydrodynamic interactions.

DIFFUSION IN CONFINED SYSTEMS

Measurement of translational diffusion in confined spaces provides apparent diffusion coefficients that can contain contributions from multiple components with different diffusion rates, transport rates between different compartments and boundary effects.

Boundary effects become important when the size of the compartments is comparable to the root-mean square displacement of the diffusing species given by

$$< z^2 >^{-2} = (2Dt)^{1/2} \tag{16}$$

For water at 25°C and a typical diffusion time of 100 ms, the distance is of the order of 20 μm. For macromolecules of the size that can be measured by NMR methods this distance can be reduced by at most two orders of magnitude and remain comparable to the size of subcellular structures. Restricted diffusion can be investigated by comparing the apparent diffusion coefficient measured with different values of the diffusion time (Tanner, 1983).

Cerdan and coworkers (García-Pérez *et al.*, 1999) have measured the apparent diffusion coefficients of several metabolites in rat erythrocytes, chicken erythrocytes and rat liver mitochondria. For lactate and ergothioneine they found a diffusional barrier of 2.5–3 μm, close to the transverse section across rat erythrocytes, but no apparent barrier was found for water or externally supplied imidazol-1-ylacetic acid. Cell membranes are highly permeable to both compounds. A quantitative interpretation of signal attenuation in PGSE experiments of complex systems is complicated by the fact that a number of different combinations of relevant parameters (compartment lengths, barrier permeabilities, diffusion and relaxation rates in each compartment are predicted to give very similar attenuation curves (Novikov *et al.*, 1998).

One of the consequences of confinement in anisotropic matrices is anisotropic diffusion. In general, diffusion in

biological tissues is anisotropic and the full diffusion tensor has to be determined. This is possible with the use of orthogonal field gradients (Basser *et al.*, 1994). This fact is used in MRI studies, for example to locate axon-fiber tracks (Baser *et al.*, 2000). Anisotropic water diffusion also been detected in tendons (Klein *et al.*, 2003).

Anisotropic diffusion can also be relevant when studying matrices that are oriented by the spectrometer magnetic field (Kuchel *et al.*, 2000) measured water diffusion anisotropy in human erythrocytes that, due to their biconcave shape, become aligned in magnetic fields. Anisotropic diffusion of small molecules has been used to study the morphology of liquid crystalline phases used to orient biological molecules (Gaemers and Bax, 2001).

CROWDING AND MOLECULAR ORDER DETECTED BY NMR

Interaction with oriented particles results in non-isotropic equilibrium distribution of molecular orientations that can be detected by the non-complete average of tensorial interactions, such as dipole–dipole interactions. Residual dipolar couplings have become a widely used tool for macromolecular structure refinement. For reviews see, for example, Prestegard *et al.* (2000); Bax *et al.* (2001); De Alba and Tjandra (2002).

Orientation induced by steric interactions is directly related to excluded volume effects and can be calculated successfully from the known three-dimensional structure of the molecule of interest (Zweckstetter and Bax, 2000; Fernandes *et al.*, 2001; Azurmendi and Bush, 2002, Almond and Axelsen, 2002). Residual orientation can also be determined by electrostatic interactions with the alignment medium (Hansen *et al.*, 1998; Clore *et al.*, 1998; Sass *et al.*, 1999), a situation which also occurs in crowded systems.

An explicit linkage between crowding and molecular orientation is provided by stretched or compressed polyacrilamide gels in which proteins become oriented (Tycko *et al.*, 2000). Diffusional properties of proteins in polyacrylamide gels have been determined. As in other crowded systems, a substantial decrease in the translational diffusion coefficient is observed (around 5-fold for ubiquitin in 10% polyacrylamide). However, the isotropic rotational correlation time is only increased from 5 to 7–8 ns. (Sass *et al.*, 2000). Electrostatic interactions with oriented systems can result in anisotropic rotation that can be detected by changing the overall orientation of the aligning system with respect to the magnetic field (Bernadó *et al.*, 2002a).

MACROMOLECULAR ASSOCIATION AND NMR

For sensitivity reasons, NMR studies are usually carried out at concentrations in the millimolar range, often much larger than the physiological concentration of the molecule of interest. The need for high concentrations sometimes introduces solubility or aggregation problems and is seen, in general, as a caveat for the assessment of the biological relevance of functional data derived from NMR. On the other hand, the total macromolecular concentration in the cell is still much higher than the one used in NMR samples and, when excluded volume effects are important, they are more likely to be detected by NMR than by other techniques that use much lower concentrations.

Several NMR parameters are sensitive to macromolecular association (Zuiderweg, 2002). One of the most extensively used methods is chemical shift perturbation mapping in which the H-^{15}N-HSQC spectrum of a labelled protein is monitored during a titration with an unlabelled species. For short-lived complexes, a single set of signals is observed along the titration and the average chemical shift changes reflect the relative populations of free and bound forms. For long-lived complexes, different sets of signals are observed for free and bound species and the relative intensities of the two sets reflect the relative populations. Intermediate exchange rates result is broadened signals. Shift perturbations are often localized in the interface, unless complexation has an effect on the conformation of the complete protein. Quantification of changes and structural interpretation beyond the identification of the interaction region is difficult.

Macromolecular association has a strong effect in the rotational correlation time. Heteronuclear NMR relaxation times of well structured regions are a sensitive measure of global molecular tumbling. The power of relaxation measurements is enhanced by the fact that macromolecular association is sensed by the complete molecule, not just the interface region. The combination of the two factors makes relaxation measurements a very promising tool to study weak association in dilute solutions, which probably reflect strong association under crowding conditions.

A recent example from our group, in collaboration with M. Akke (University of Lund), illustrates this idea (Bernadó *et al.*, 2003). Low molecular weight bovine protein tyrosin phosphatase (BPTP, MW 18 kDa) was known to be present in solution as an equilibrium mixture of a monomer and a

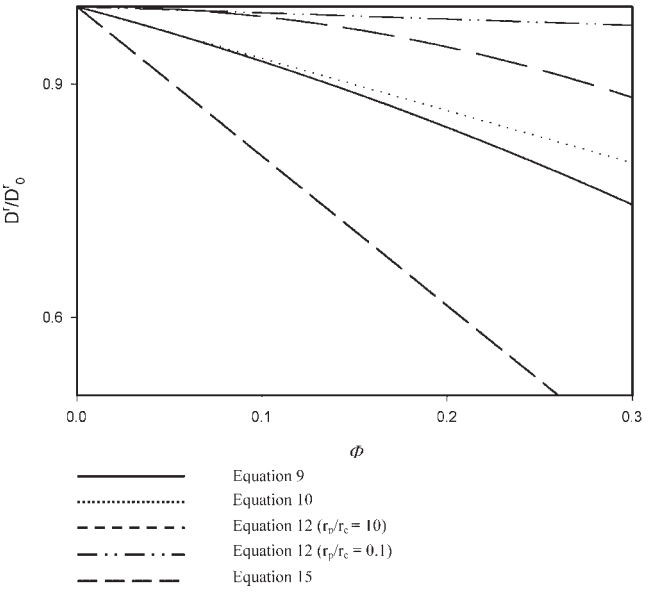

Figure 3. Reduced rotational diffusion coefficients according to the models discussed in the text. Equations (9) (10) and (15) are for monodisperse suspensions of spheres. Equation (15) assumes strongly charged spheres. Equations 12 is plotted for a sphere much larger ($\lambda = 10$) or smaller than the crowder ($\lambda = 0.1$).

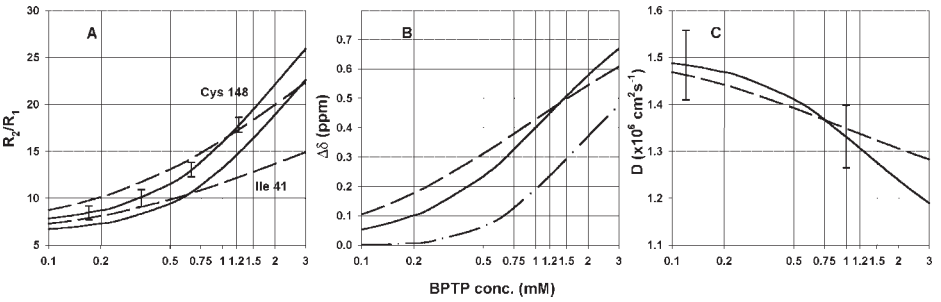

Figure 4. Calculated concentration dependence of different NMR observables for the BPTP system, assuming the monomer–dimer–tetramer model (continuous lines) and a simpler monomer–dimer model (dashed lines). (A) Backbone nitrogen R_2/R_1 for residues I41 and C148. Uncertainties are indicated at four different concentrations for C148. These are average experimental errors considering all used residues and are also applicable to I41. (B) Average chemical shift, assuming a chemical shift difference of 1 ppm between monomer and dimer sites but no chemical shift difference between dimer and tetramer. The dot–dash curve has been calculated, assuming a monomer–dimer–tetramer model with a 1 ppm difference between dimer and tetramer sites but no difference between monomer and dimer. (C) Translational diffusion coefficient. Error bars represent a relative uncertainty of 5%. Reprinted with permission from Bernadó *et al.* 2003. Copyright 2003 American Chemical Society.

dimer. Concentration-dependent relaxation time measurements showed a substantial amount of a previously unknown tetramer, formed by interaction between two dimers. Identification of individual residues forming a well defined interface was taken as evidence for the formation of a specific oligomer, rather than non-specific aggregation. Based on structural data we have suggested a regulatory role for BPTP tetramers analogous to the one played by inactive proenzymes, except for its reversibility. For such a regulatory mechanism to be effective, the association constant should be comparable to the effective concentration, i.e. the thermodynamic activity, of BPTP in its natural medium. Excluded volume effects result in effective concentrations in the cytoplasm that are much larger than the nominal ones. When the same process is studied in dilute solution, the apparent association constant may be much lower and would be detected as a weak association by NMR but could go undetected by other techniques that require lower concentrations. The effect of crowding on the modulation of the activity of a different enzyme (glyceraldehyde-3-phosphate dehydrogenase) by tetramerization has been described (Minton and Wilf, 1981).

Figure 4 compares the ability of different NMR-based techniques to differentiate between alternative association mechanisms in the BPTP example: relaxation time measurements, chemical shift perturbation and translational diffusion. In the particular example studied, where at the highest BPTP concentration studied the mole fraction of protein in the tetramer form is around 0.3, only relaxation time measurements had adequate precision to separate the monomer–dimer from the monomer–dimer–tetramer models. Excluded volume effects are especially noticeable in the formation of higher oligomers (i.e tetramers) of macromolecules. It has been suggested that the shift in the tetramerization equilibrium of a 40 kD protein between the *E. coli* cytoplasm and a diluted solution can be as high as 10^3–10^5 (Ellis, 2001b).

CONCLUDING REMARKS

Macromolecular crowding is a general phenomenon in biological systems and has strong thermodynamic and kinetic consequences. NMR is a versatile tool that can be used to monitor several parameters affected by macromolecular crowding. Rotational diffusion is the main determinant of NMR relaxation rates and line widths. Hydrodynamic models of crowded systems provide working models for the simplest case of macromolecular crowding, involving hard spheres. In particular, hydrodynamic models explain the different effects of crowding on translational and rotational diffusion. Rotational diffusion is only weakly affected by crowding conditions. This has opened the possibility of studying proteins overexpressed in living cells. NMR relaxation is a sensitive monitor of macromolecular association. Weak specific oligomerization detected by NMR relaxation in dilute solutions may be biologically relevant as an indication of extensive *in vivo* oligomerization promoted by cellular crowding.

Acknowledgements

This work was supported by funds from the Spanish Ministerio de Ciencia y Tecnología (BIO2001-3115 and BQU2003-04517) and the Generalitat de Catalunya (to M.P.). P.B is a recipient of a European Molecular Biology Organization postdoctoral fellowship.

REFERENCES

Almond A, Axelsen JB. 2002. Physical interpretation of residual dipolar couplings in neutral aligned media. *J. Am. Chem. Soc.* **124**: 9986–9987.

Antosiewicz J, McCammon JA. 1995. Electrostatic and hydrodynamic orientational steering effects in enzyme–substrate association. *Biophys. J.* **69**: 57–65.

Azurmendi HF, Bush CA. 2002. Tracking alignment from the moment of inertia tensor (TRAMITE) of biomolecules in neutral dilute liquid crystal solutions. *J. Am. Chem. Soc.* **124**: 2426–2427.

Basser PJ, Mattiello J, LeBihan, D. 1994. Estimation of the effective self-diffusion tensor from the NMR spin echo. *J. Magn. Reson. B* **103**: 247–254.

Basser PJ, Pajevic S, Pierpaoli C, Duda J, Aldroubi A. 2000. *In vivo* fiber tractography using DT-MRI data. *Magnetic Reson. Med.* **44**: 625–632.

Bax A, Kontaxis A, Tjandra N. 2001. Dipolar couplings in macromolecular structure determination. *Methods in Enzym.* **339**: 127–174.

Bernadó P, Barbieri R, Padrós E, Luchinat C, Pons M. 2002a. Lanthanide modulation of the orientation of macromolecules induced by purple membrane. *J. Am. Chem. Soc.* **124**: 374–375.

Bernadó P, García de la Torre J, Pons M. 2002b. Interpretation of ^{15}N NMR relaxation data of globular proteins using hydrodynamic calculations with HYDRONMR. *J. Biomol. NMR* **23**: 139–150.

Bernadó P, Åkerud T, García de la Torre J, Akke M, Pons M. 2003. Combined use of NMR relaxation measurements and hydrodynamic calculations to study protein association: evidence for tetramers of low molecular weight protein tyrosine phosphatase in solution. *J. Am. Chem. Soc.* **125**: 916–923.

Bicknese S, Periasamy N, Shohet SB, Verkman AS. 1993. Cytoplasmic viscosity near the cell plasma membrane: measurement by evanescent field frequency-domain microfluorimetry. *Biophys. J.* **65**: 1272–1282.

Brune D, Kim S. 1994. Hydrodynamic steering effects in protein association *Proc. Natl Acad. Sci. USA* **91**: 2930–2934.

Cichocki B, Ekiel-Jezewska ML, Wajnryb E. 1999. Lubrication corrections for three-particle contribution to short-time self-diffusion coefficients in colloidal dispersions. *J. Chem. Phys.* **111**: 3265–3273.

Clore GM, Starich MR, Gronenborn AM. 1998. Measurement of residual dipolar couplings of macromolecules aligned in the nematic phase of a colloidal suspension of rod-shaped viruses. *J. Am. Chem. Soc.* **120**: 10571–10572.

Dayel MJ, Hom EFY, Verkman AS. 1999. Diffusion of green fluorescent protein in the aqueous-phase lumen of endoplasmic reticulum. *Biophys. J.* **76**: 2843–2851.

Dayie KT, Wagner G, Lefèvre, J-F. 1996. Theory and practice of nuclear spin relaxation in proteins. *A. Rev. Phys. Chem.* **47**: 243–282.

De Alba E, Tjandra N. 2002. NMR dipolar couplings for the structure determination of biopolymers in solution. *Prog. NMR spectrosc.* **40**: 175–197.

Dedmon MM, Patel CN, Young GB, Pielak GJ. 2002. FlgM gains structure in living cells. *Proc. Natl Acad. Sci. USA* **99**: 12681–12684.

Degiorgio V, Piazza R. 1995. Rotational diffusion in concentrated colloidal dispersions of hard spheres. *Phys. Rev. E* **52**: 2707–2717.

Demco DE, Johansson A, Tegenfeldt J. 1994. Constant-relaxation methods for diffusion measurements in the fringe field of superconducting magnets *J. Magn. Reson. A* **110**: 183–193.

Dhont JKG. 1996. *An Introduction to the Dynamics of Colloids*, Chap. 6. Elsevier: Amsterdam.

Ellis RJ. 2001a. Macromolecular crowding: obvious but underappreciated. *Trends Biochem Sci.* **26**: 597–604.

Ellis RJ. 2001b. Macromolecular crowding: an important but neglected aspect of the intracellular environment. *Curr. Opin. Struct. Biol.* **11**: 114–119.

Endre ZH, Chapman BE, Kuchel PW. 1983. Intra-erythrocyte microviscosity and diffusion of specifically labelled [glycyl-alpha-13C]glutathione by using 13C n.m.r. *Biochem. J.* **216**: 655–660.

Fernandes MX, Bernadó P, Pons M, de la Torre JG. 2001. An analytical solution to the problem of the orientation of rigid particles by planar obstacles: application to membrane systems and to the calculation of dipolar couplings in protein NMR spectroscopy. *J. Am. Chem. Soc.* **123**: 12037–12047.

Ferrage F, Zoonens M, Warschawski DE, Popot J-L, Bodenhausen G. 2003. Slow diffusion of macromolecular assemblies by a new pulsed field gradient NMR method. *J. Am. Chem. Soc.* **125**: 2541–2545.

Fushimi K, Verkman AS. 1991. Low viscosity in the aqueous domain of cell cytoplasm measured by picosecond polarization microfluorometry. *J. Cell Biol.* **112**: 719–725.

Gaemers S, Bax A. 2001. Morphology of three liquid crystalline biological NMR media studied by translational diffusion anisotropy. *J. Am. Chem. Soc.* **123**: 12343–12352.

García de la Torre J, Huertas ML, Carrasco B. 2000. HYDRONMR: prediction of NMR relaxation of globular proteins from atomic-level structures and hydrodynamic calculations. *J. Magn. Reson.* **147**: 138–146.

García-Pérez AI, López-Beltran EA, Klüner P, Luque J, Ballesteros P, Cerdan S. 1999. Molecular crowding and viscosity as determinants of translational difusión of metabolitos in subcellular organelles. *Arch. Biochem. Biophys.* **362**: 329–338.

Håkansson B, Jönsson B, Linse P, Söderman O. 1977. The influence of a nonconstant magnetic-field gradient on pfg nmr diffusion experiments: a Brownian-dynamics computer simulation study. *J. Magn. Reson.* **124**: 343–351.

Han J, Herzfeld J. 1993. Macromolecular diffusion in crowded solutions. *Biophys. J.* **65**: 1155–1161.

Hanna S, Hess W, Klein R. 1982. Self-diffusion of spherical brownian particles with hard-core interactions. *Phys. A.* **111**: 181–199.

Hansen MR, Müller L, Pardi A. 1998. Tunable alignment of macromolecules by filamentous phage yields dipolar coupling interactions. *Nat. Struct. Biol.* **5**: 1065–1074.

Imhof A, Dhont JKG. 1995. Long-time self-diffusion in binary colloidal hard-sphere dispersions. *Phys. Rev. E* **52**: 6344–6357.

Johnson CS Jr. 1999. Diffusion ordered nuclear magnetic resonance spectroscopy: principles and applications. *Prog. NMR Spectrosc.* **34**: 203–256.

Jones RB. 1989. Rotational diffusion of a tracer colloid particle—II: long time orientational correlations. *Phys. A* **157**: 752–768.

Klein M, Fechete R, Demco DE, Blümich B. 2003. Self-diffusion measurements by a constant-relaxation method in strongly inhomogeneous magnetic fields. *J. Magn. Reson.* **164**: 310–320.

Koenderink GH, Zhang H, Aarts DGA, Lettinga MP Philipse AP, Nägele G. 2003. On the validity of Stokes–Einstein–Debye relations for rotational diffusion in colloidal suspensions. *Faraday Disc.* **123**: 335–354.

Korzhnev DM, Billeter M, Arseniev AS, Orekhov VY. 2001. NMR studies of Brownian tumbling and internal motions in proteins. *Prog. NMR Spectrose* **38**: 197–266.

Kuchel PW, Chapman BE. 1993. Heteronuclear Double-Quantum-Coherence Selection with Magnetic-Field Gradients in Diffusion Experiments. *J. Magn. Reson. A* **101**: 53–59.

Kuchel PW, Durrant CJ, Chapman BE, Jarrett PS, Regan DG. 2000. Evidence of red cell alignment in the magnetic field of an NMR spectrometer based on the diffusion tensor of water. *J. Magn. Reson.* **145**: 291–301.

Lipari G, Szabo A. 1982a. Model-free approach to the interpretation of nuclear magnetic resonance relaxation in macromolecules—1: theory and range of validity. *J. Am. Chem. Soc.* **104**: 4546–4559.

Lipari G, Szabo A. 1982b. Model-free approach to the interpretation of nuclear magnetic resonance relaxation in macromolecules—2: analysis of experimental results. *J. Am. Chem. Soc.* **104**: 4559–4570.

Livingston DJ, La Mar GN, Brown WD. 1983. Myoglobin diffusion in bovine heart muscle. *Science* **220**: 71–73.

Luby-Phelbs K. 1994. Physical properties of cytoplasm. *Curr. Opin. Cell Biol.* **6**: 3–9.

Luby-Phelbs KS, Mujumdar S, Mujumdar RB, Ernst LA, Galbraith W, Waggoner AS. 1993. A novel fluorescence ratiometric method confirms the low solvent viscosity of the cytoplasm. *Biophys. J.* **65**: 236–242.

Mastro AM, Babich MA, Taylor WD, Keith AD. 1984. Diffusion of a small molecule in the cytoplasm of mammalian cells. *Proc. Natl Acad. Sci. USA* **81**: 3414–3418.

Minton AP, Wilf J. 1981. Effect of macromolecular crowding upon the structure and function of an enzyme: glyceraldehyde-3-phosphate dehydrogenase. *Biochemistry* **20**: 4821–4826.
Novikov EG, van Dusschoten D, Van As H. 1998. Modeling of self-diffusion and relaxation time NMR in multi-compartment systems. *J. Magn. Reson.* **135**: 522–528.
Palmer AG. 2001. Nmr probes of molecular dynamics: overview and comparison with other techniques. *A. Rev. Biophys. Biomol. Struct.* **30**: 129–155.
Palmer AG. Kroenke CD Loria JP. 2001. Nuclear magnetic resonance methods for quantifying microsecond-to-millisecond motions in biological macromolecules. *Meth. Enzym.* **339**: 204–238.
Pervushin K. 2000. Impact of transverse relaxation optimized spectroscopy (TROSY) on NMR as a technique in structural biology. *Q. Rev. Biophys.* **33**: 161–197.
Pervushin K, Riek R, Wider G, Wüthrich K. 1997. Attenuated T_2 relaxation by mutual cancellation of dipole-dipole coupling and chemical shift anisotropy indicates an avenue to NMR structures of very large biological macromolecules in solution. *Proc. Natl Acad. Sci. USA* **94**: 12366–12371.
Prestegard JH, Al-Hashimi HM, Tolman JR. 2000. NMR structures of biomolecules using field oriented media and residual dipolar couplings. *Q. Rev. Biophys* **33**: 371–424.
Price WS. 2000. NMR gradient methods in the study of proteins. *A. Rep. Prog. Chem. C* **96**: 3–53.
Sass J, Cordier F, Hoffmann M, Rogowski M, Cousin A, Omichinski JG, Löwen H, Grzesiek S. 1999. Purple Membrane Induced Alignment of Biological Macromolecules in the Magnetic Field. *J. Am. Chem. Soc.* **121**: 2047–2055.
Sass J, Musco G, Stahl SJ, Wingfield PT, Grzesiek S. 2000. Solution NMR of proteins within polyacrylamide gels: diffusional properties and residual alignment by mechanical stress or embedding of oriented purple membranes. *J. Biomol. NMR* **18**: 303–309.
Serber Z, Dötsch V. 2001. In-cell NMR spectroscopy. *Biochemistry* **40**: 14317–14323.
Spiess HW. 1991. Structure and dynamics of solid polymers from 2D- and 3D-NMR *Chem. Rev.* **91**: 1321–1338.
Stejskal EO, Tanner JE. 1965. Spin diffusion measurements: spin echoes in the presence of a time-dependent field gradient. *J. Chem. Phys* **42**: 288–292.
Tanner JE. 1970. Use of the stimulated echo in NMR diffusion studies. *J. Chem. Phys* **52**: 2523–2526.
Tanner JE. 1983. Intracellular diffusion of water. *Arch. Biochem. Biophys.* **224**: 416–428.
Tillett ML, Horsfield MA, Lian L-Y, Norwood TJ. 1999. Protein–ligand interactions measured by 15N-filtered diffusion experiments *J. Biomol. NMR.* **13**: 223–232.
Tokuyama M, Oppenheim I. 1994. Dynamics of hard-sphere suspensions. *Phys. Rev. E* **50**: 16–19.
Tugarinov V, Hwang PM, Ollerenshaw JE, Kay LE. 2003. Cross-correlated relaxation enhanced ^{1}H-^{13}C NMR spectroscopy of methyl groups in very high molecular weight proteins and protein complexes. *J. Am. Chem. Soc.* **125**: 10420–10428.
Tycko R, Blanco FJ, Ishii Y. 2000. Alignment of biopolymers in strained gels: a new way to create detectable dipole–dipole couplings in high-resolution biomolecular NMR *J. Am. Chem. Soc.* **122**: 9340–9341.
van Blaaderen, Peetermans AJ, Maret G, Dhont JKG. 1992. Long-time self-diffusion of spherical colloidal particles measured with fluorescence recovery after photobleaching *J. Chem. Phys.* **96**: 4591–4603.
van Megen W, Underwood SM. 1989. Tracer diffusion in concentrated colloidal dispersions—III: mean squared displacements and self-diffusion coefficients. *J. Chem. Phys.* **91**: 552–559.
Von Meerwall E, Kamat M. 1989. Effect of residual field gradients on pulsed-gradient NMR diffusion measurements *J. Magn. Reson.* **83**: 309–323.
Watzlawek M, Nägele G. 1997. Short-time rotational diffusion in monodisperse charge-stabilized colloidal suspensions. *Physica A* **235**: 56–74.
Wieruszeski J-M, Bohin ABohin J-P, Lippens G. 2001. *In vivo* detection of the cyclic osmoregulated periplasmic glucan of *Ralstonia solanacearum* by high-resolution magic angle spinning NMR. *J. Magn. Reson.* **151**: 118–123.
Williams SP, Haggie PM, Brindle KM. 1997. ^{19}F NMR measurements of the rotational mobility of proteins *in vivo*. *Biophys. J.* **72**: 490–498.
Zhang H, Nägele G. 2002. Tracer-diffusion in binary colloidal hard-sphere suspensions *J. Chem. Phys.* **117**: 5908–5920.
Zimmerman SB, Minton AP. 1993. Macromolecular crowding: biochemical, biophysical, physiological consequences. *A. Rev. Biophys. Biomol. Struct.* **22**: 27–65.
Zimmerman SB, Trach SO. 1991. Estimation of macromolecule concentrations and excluded volume effects for the cytoplasm of *Escherichia coli*. *J. Mol. Biol.* **222**: 599–620.
Zuiderweg ERP. 2002. Mapping protein–protein interactions in solution by NMR spectroscopy. *Biochemistry* **41**: 1–7.
Zweckstetter M, Bax A. 2000. Prediction of sterically induced alignment in a dilute liquid crystalline phase: aid to protein structure determination by NMR. *J. Am. Chem. Soc.* **122**: 3791–3792.

APPENDIX: TWO TIME REGIMES IN THE HYDRODYNAMICS OF DENSE (CROWDED) SYSTEMS

Here we estimate the characteristic time between collisions, τ_{col}. We consider only the simple but significant case in which all particles are spherical. An easy approach is feasible neglecting HI interaction effects; then, the kinetics of the encounters between particles can be described in terms of the Smoluchowski theory of diffusion controlled reactions. Let us restrict the description to the case in which there are only two types of particles: the 'test' particles, P, and the 'crowder', C. As we learn from standard textbooks, the rate law of a reaction which is solely controlled by diffusion (i.e. when in addition to absence of HI, there is no energetic–electrostatic, etc. interaction):

$$P + C \rightarrow X \tag{A1}$$

is given by

$$V = d[X]/dt = k[P][C] \tag{A2}$$

Smoluchowski showed that, under those assumptions, the second-order (molar) rate constant k is:

$$k = 4\pi\sigma D_{PC} N_A \tag{A3}$$

where N_A is the Avogadro number. σ is the interparticle distance at which reaction occurs, that is assimilated to the collision distance between the hard spheres, equal to the sum of the two radii, $\sigma = r_P + r_C$. D_{PC} is the diffusion coefficient of one particle with respect to the other one, which in the absence of HI is just the sum of the individual diffusion coefficient, given by the Stokes–Einstein equation for spheres:

$$D_{PC} = D_P + D_C = (k_B T/6\pi\eta)(1/r_P + 1/r_C) \tag{A4}$$

where η is the solvent viscosity. Thus, the final expression for the molar rate constant is:

$$k = 4\pi N_A (k_B T/6\pi\eta)(r_P + r_C)(1/r_P + 1/r_C) \tag{A5}$$

Similary, the rate can be expressed in terms of the number concentrations, instead of molar concentration:

$$V' = dn_X/dt = k' n_P n_C \quad (A6)$$

where $n_C = [C]N_A$ and therefore $k' = k/N_A$.

V' is equivalent to the number of collisions of C molecules with P molecules per unit volume and unit time. There are n_P test particles per unit volume, so that the number of collisions of one P particle with C particles, or in other words, the frequency of P–C collisions, is $f_{col} = V'/n_P$. Finally, the characteristic time between collision is expressed (as they would occur at equal intervals) as $\tau_{col} = 1/f_{col}$ and therefore we have

$$\tau_{col} = [4\pi(k_B T/6\pi\eta)(r_P + r_C)(1/r_P + 1/r_C)n_C]^{-1} \quad (A7)$$

The amount of the crowding effect is usually expressed as the volume fraction occupied for the P and C particles, ϕ; the remainder is free volume. We assume that the test particles are diluted and the volume that they all occupy is much smaller than that of the crowder particles. Then the number concentration and the occupied volume fraction are related through $n_C = \phi/v_C$, where $v_C = 4\pi r_C^3/3$ is the volume of the spherical crowders. Thus the characteristic collision time is finally given by:

$$\tau_{col} = [3(k_B T/6\pi\eta)(r_P + r_C)(1/r_P + 1/r_C)\phi]^{-1} r_C^3 \quad (A8)$$

This time can be compared with characteristic times of (free) translational and rotational Brownian motion of the test particles. For translation, the characteristic time can be defined as the time for which the root-mean-square displacement is the same as the particle size, represented by the spherical radius. The relationship is $r_P^2 = 6(k_B T/6\pi\eta r_P)\tau_{trans}$ so that $\tau_{trans} = \pi\eta r_P^3/k_B T$. For rotation, the characteristic time is the Debye rotational (correlation) time of the spherical particle, $\tau_{trans} = 4\pi\eta r_P^3/3k_B T$. It is evident that these two times are quite similar. We will take for reference the translational one, which is hereafter denoted as the P particle's characteristic time, $\tau_{part} = \pi\eta r_P^3/k_B T$.

As mentioned above, the first regime takes place when the collision time is much larger than the particle's own time, $\tau_{col} \gg \tau_{part}$, or when $\tau_{part}/\tau_{col} \ll 1$. Interestingly, the ratio is proportional to the occupied volume fraction, and the proportionality constant is a simple function of the ratio of radii, $\lambda = r_P/r_C$:

$$\tau_{part}/\tau_{col} \approx \phi F(\lambda)$$

where

$$F(\lambda) = (1/2)(1 + \lambda)(1 + \lambda^{-1})\lambda^3$$